A microfluidic platform for integrated synthesis and dynamic light scattering measurement of block copolymer micelles†

Thomas Q. Chastek,‡ Kazunori Iida,‡ Eric J. Amis,* Michael J. Fasolka and Kathryn L. Beers

Received 27th November 2007, Accepted 13th March 2008
First published as an Advance Article on the web 1st May 2008
DOI: 10.1039/b718235j

Microfluidic devices were developed that integrate the synthesis of well defined block copolymers and dynamic light scattering (DLS) measurement of their micelle formation. These metal devices were designed to operate in contact with organic solvents and elevated temperatures for long periods, and thus were capable of continuous in-channel atom transfer radical polymerization (ATRP) of styrene and (meth)acrylate homopolymers and block copolymers. These devices were equipped with a miniaturized fiber optic DLS probe that included several technology improvements, including a measurement volume of only 4 microlitres, simple alignment, and reduced multiple scattering. To demonstrate the integrated measurement, poly(methyl methacrylate-*b*-lauryl methacrylate) and poly(methyl methacrylate-*b*-octadecyl methacrylate) block copolymers were processed on the device with a selective solvent, dodecane, to induce micelle formation. The *in situ* DLS measurements yielded the size and aggregation behavior of the micelles. For example, the block copolymer solutions formed discrete micelles ($D_H \approx 25$ nm) when the corona block was sufficiently long ($f_{MMA} < 0.51$), but the micelles aggregated when this block was short. This study demonstrates the utility of these new devices for screening the solution behavior of custom synthesized polymeric surfactants and additives.

1. Introduction

Microfluidic technology directed towards polymeric materials is expected to have a broad impact given the ubiquity of polymer additives in such things as coatings, personal care products, and pharmaceuticals. Miniaturized and integrated synthesis and analysis of these polymer additives can play an important role in accelerating the screening of often complex structure–property relationships, related to key attributes such as wear resistance, optical clarity, and triggered molecule delivery.[1–3] Some work in applying microfluidics to polymers has focused on harnessing specific microchannel and flow designs to create uniquely structured micron-scale polymeric particles.[4,5] There has been little attention, however, on integrated microfluidic synthesis and analysis systems for polymer materials. One limitation is that common synthetic polymers are not well suited for evaluation with many existing microfluidic analysis techniques, such as electrophoresis and fluorescence spectroscopy.[6–8] Some recent studies, however, have characterized polymers within microfluidic environments by monitoring parallel flow streams to determine the molecular mass[9] and viscosity[10] of polymer containing samples.

When dealing with polymer laden fluids, one fundamental concern is the assembly and interaction of the polymer chains. A few microfluidic analysis techniques have been directed at characterizing such nanoscale structure, including small angle light scattering,[11] and fluorescence correlation spectroscopy.[12,13] On the other hand, in traditionally sized measurements, dynamic light scattering (DLS) has been established as a powerful tool for *in situ* size analysis of sub-micrometre polymer assemblies.[14] Recent work in our lab has outlined methods for incorporating DLS into miniaturized devices through fiber optic probes.[15] The fiber optic DLS was demonstrated on stock solutions of block copolymer micelles, and quantitative measurement of micelles as small as 10 nm in diameter was found to be straightforward.

Additionally, previous reports from this laboratory have examined microfluidic polymer synthesis, specifically, aqueous-based atom transfer radical polymerizations (ATRP). The thrust of this work was the application of microfluidic ATRP to sequential high-throughput polymer library production.[16,17] It was found that ATRP conducted within microchannels have kinetics and product molecular weights similar to those obtained in batch reactors. These studies were carried out in thiolene-based devices, which like poly(dimethylsiloxane)[18,19] (PDMS) and thermoplastic-based[20] devices, offer advantages such as low cost and transparency, allowing for optical microscopy and spectroscopy analyses. These devices, however, are not suitable for the many common polymer syntheses that are conducted under harsh conditions. For example, PDMS devices swell in many organic solvents[21] and are permeable to oxygen, whereas thiolene-based devices can leak and delaminate when in contact with heated organic solvents for extended periods of time. On the other hand, stainless steel micromixers and tubing

Polymers Division, National Institute of Standards and Technology, 100 Bureau Drive MS8542, Gaithersburg, Maryland 20899, USA. E-mail: thomas.chastek@nist.gov, eric.amis@nist.gov; Fax: +1-(301)-975-4924; Tel: +1-(301)-975-4671

† Electronic supplementary information (ESI) available: GPC traces of a PMMA-Br macroinitiator and PMMA-*b*-PLMA diblock copolymers obtained by microfluidic polymerization. See DOI: 10.1039/b718235j

‡ Both authors contributed equally to this work.

microreactors, have proven to be a robust route for miniaturized polymer syntheses.[22–27] However, they often lack some benefits generally associated with microfluidic devices, such as the ability to integrate complex flow designs and characterization tools into a small semi-disposable device.

In this paper, we report on a new metal-based microfluidic device that integrates synthesis of block copolymers and *in situ* nanoscale structure measurements *via* DLS. These devices are simple and inexpensive to manufacture, and are demonstrated to be compatible with ATRP syntheses of well defined commonly used polymers, such as polystyrene (PS) and several poly(meth)acrylates. Synthesis of homopolymers and block copolymers were carried out at elevated temperatures in organic solvents, with no observed detriment to the microfluidic devices. The flow path was used to dilute the block copolymers with a selective solvent, thereby inducing micelle formation. The size and size distribution of the self-assembled polymers were determined by integrated dynamic light scattering (DLS). A depiction of the overall device is presented in Fig. 1.

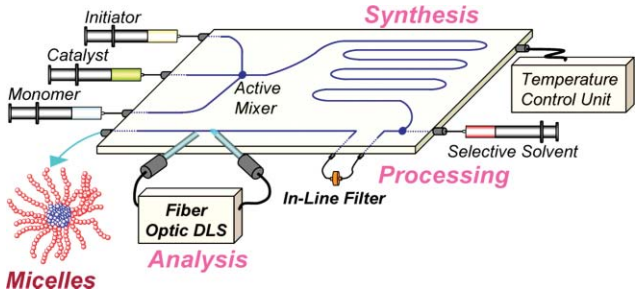

Fig. 1 Shown is a scheme of the microfluidic system that integrates ATRP synthesis of diblock copolymers, micellization, and *in situ* nanoscale particle sizing with dynamic light scattering.

2. Microfluidic device production

Microfluidic reactors used for polymer synthesis need to be stable in hot organic solvents and accommodate relatively high viscosities. Small molecule organic synthesis is often conducted within glass devices, which are prepared with photolithography and thermal bonding methods.[28] Our devices follow the same conceptional design (*i.e.*, creating channels then sealing), but with wider channels to accommodate the somewhat higher viscosity of the polymer samples. Also, the larger channels make metal an appealing substrate, since it can be machined at these dimensions with common tools.

Our microfluidic devices consist of channels machined into an aluminium plate (7.6 cm × 10.1 cm × 1 cm). A machined aluminium block is pictured in Fig. 2a,b. The microchannels were sealed by attaching Kapton film (130 μm thick) to the aluminium surface with chemically resistant epoxy. An example of a sealed device is pictured in Fig. 2d. All of the materials were chosen due to their chemical stability and compatible thermal expansion coefficients. Kapton is also sufficiently transparent to visualize the flow and verify proper attachment.

Machining metal substrates provides several advantages. For example, threaded air tight ports can be machined into the metal substrate, and thermocouples and heating cartridges (3.2 mm diameter, 5 cm length, Watlow Firerod) can be embedded to provide good temperature control (±0.3 °C).[29] In this work, channels were typically 790 μm wide and 790 μm deep, which were easily and inexpensively prepared using a standard computer numerically controlled (CNC) milling machine. For example, the channel can be cut out with a 790 μm diameter solid carbide endmill (McMaster Carr 8795A121). In general, production of increasingly narrower channels on metal substrates requires increasingly sophisticated tools and techniques,[30] and at

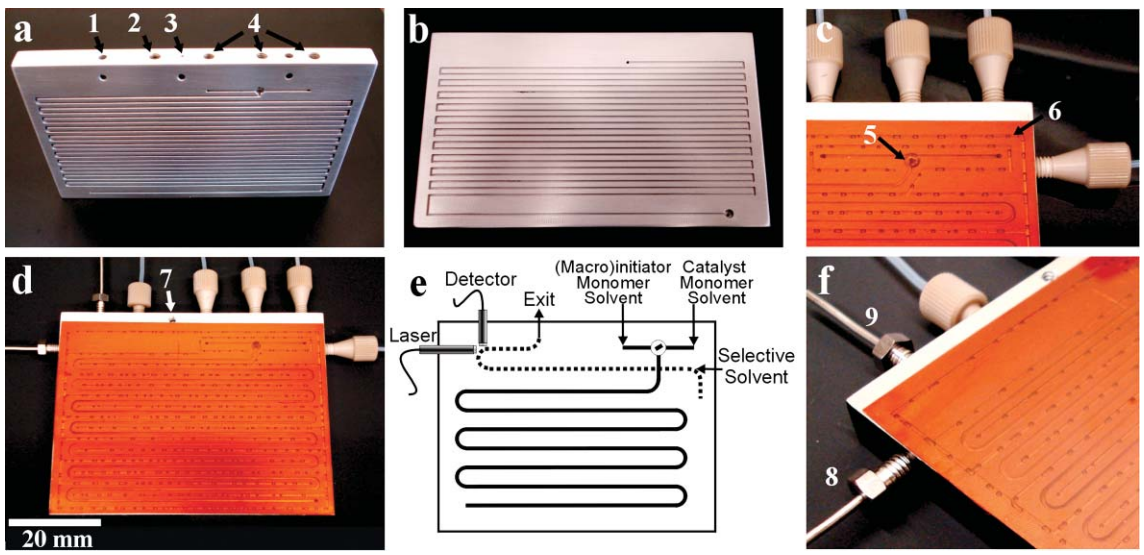

Fig. 2 Shown are images of two example microfluidic devices, one unsealed and the other sealed. (a,b) An unsealed device without integrated DLS probes is shown from different angles. (c,d) A sealed device with integrated DLS probes. Image (c) highlights the presence of a mixing well with miniature stir bar. (e) A schematic corresponding to the sealed microfluidic device. The solid line depicts the channel on the top surface of the device, and the dashed line partially depicts only the end segment of the channel on the interior of the device. For simplicity, not all channels are depicted. (f) A closer view of the DLS probes. Additional labeled features include, (1) hole for heating cartridge, (2) exit, (3) hole for thermocouple, (4) reagent inlets, (5) mixing well with miniature stir bar, (6) channel for holding glue, (7) holes for set screws used to secure the heating cartridges and thermocouple, (8) laser probe, and (9) detector probe.

some length scale it becomes more convenient to etch channels into glass or silicon substrates with photolithography.

Both devices shown in Fig. 2 consist of 3 ports feeding into a mixing well. Syringes were connected to the device with Teflon tubing and standard pressure-tight HPLC fittings, as shown in Fig. 2d. A 14 μL mixing well (3.1 mm diameter, 1.75 mm deep) with an active mixing element (nickel plated neodymium magnet, 1.5 mm diameter, 1.5 mm length, K & J magnetics)[29] was used to blend the reagents. A mixing well is highlighted in Fig. 2c. The stirring rate was sufficiently fast (*ca.* 2 Hz) to ensure proper mixing at all the examined flow rates. Microchannels were made on both sides of the aluminium plate and were connected by a single 1 mm through-hole. The channel path lengths ranged from 1.5 m to 4.5 m, and the total internal volume was between 900 μL and 4000 μL. Channel lengths were selected to obtain the appropriate residence time. That is, the total flow rate was generally fixed at approximately 500 μL h^{-1} to obtain the minimal amount of material needed to conduct periodic analyses. Thus, a polymerization lasting two hours at this flow rate required a 790 μm × 790 μm × 1.6 m channel. An inlet was often included towards the end of the channel to introduce a selective solvent to induce micelle formation, as is highlighted in Fig. 2d, and schematically depicted in Fig. 2e.

The Kapton was attached to the aluminium using a solvent resistant epoxy adhesive (Master Bond EP41S-4) and cured at 50 °C for 2 h. Prior to Kapton attachment, the aluminium surfaces were oxidized by plasma oxidation (60 W, 120 s) in order to improve adhesion between the epoxy and aluminium, and to stabilize the surface. The epoxy was applied to the appropriate aluminium surfaces with a syringe, and excess glue was removed prior to attaching the Kapton. Also, it was found that the epoxy–aluminium bond was strengthened by machining additional channels (790 μm wide, 500 μm deep) to hold glue, as can be seen in Fig. 2c. The additional glue channels were not entirely filled, incorporating several trapped air bubbles. Partial filling of the glue channels was not found to be a problem. It should be noted that the devices were amenable to cleaning either through sonication or by removing then replacing the Kapton.

A key feature of these devices is their stability with respect to organic solvents and temperature. Various organic solvents were flowed through the channel, and no noticeable effect was observed in the case of anisole (90 °C/24 h), toluene (95 °C/24 h), and methylethylketone (70 °C/24 h). In addition, the devices were repeatedly washed at room temperature with chloroform, dichloromethane, acetone, and tetrahydrofuran. The only solvent tested that was observed to have an impact was dimethyl formamide (DMF). When DMF at 100 °C was used, no effect was observed for the first 3 h, but after 24 h the Kapton film noticeably warped, eventually leaking.

3. Integrated dynamic light scattering

Some devices were integrated with dynamic light scattering (DLS), which is a method for *in situ* sizing of particles as small as a few nm in solution. As implemented in this work, DLS is non-invasive, quantitative, and fast.[31] An important feature of the miniaturized DLS used in this work is that the laser and detector fiber optic probes are mounted in direct contact with the sample solution, thus negating typical problems associated with refraction. Due to this design, no refraction occurs, regardless of the angle at which the probes are mounted. The probes are closely spaced within the microchannel providing additional advantages: (1) the volume being interrogated was confined to only a 2 mm section of a 1.5 mm diameter channel resulting in a measurement volume of only 4 μL. (2) The channel remains narrow, minimizing dead volume. (3) Alignment is greatly simplified. (4) Multiple scattering is reduced, which allows for higher than typical concentrations to be interrogated.

The online fiber optic DLS, based on our previous work,[15] was integrated into several of the devices through two identical fiber optic probes, as can be seen in Fig. 2f. One was attached to a laser (Lexel 75, 488 nm, 200 mW) and the other to a photomultiplier tube (Hamamatsu HC120–08). The dark count rate of the detector was less than 50 counts per second. The detector signal was correlated with a BI-9000AT correlator. The laser light was launched into the laser probe with a fiber coupler (Newport, F1015), and the scattered light was directed out of the detector probe onto the detector with a fiber coupling (FC) connection. The probes consisted of a gradient refractive index (GRIN) lens (1 mm diameter, 2.3 mm length, NSG America) affixed to a polarization maintaining single mode optical fiber (HB450, Thorlabs).[29] The fiber and lens are housed within a 1.6 mm diameter stainless steel tube. The GRIN lenses collimate the laser light effectively producing a well defined coherence volume. Based on the calculations of Dhadwal and Chu,[32] the probes have an angular uncertainty, $(\Delta\theta)_f$, of 1.4 mrad and an effective pupil entrance, D_A, of 230 μm. Given the beam diameter of 230 μm,[15] the coherence volume is 10 nL. The DLS was periodically calibrated with latex size standards (Duke Scientific), and consistently yielded sizes accurate to within 5%. Moreover, measurements with the fiber optic DLS were frequently compared to results obtained from a full-scale DLS (Brookhaven Instruments BI-200SM), with consistently very good agreement. The detector probe was aligned at a single scattering angle of 90°. It should be noted that the detector probe can be mounted at a range of angles (*e.g.*, $30° < \theta < 150°$), as demonstrated in our previous work.[15] Multiangle measurements, however, are limited by the availability of channel surface area needed to introduce multiple probes. The micelle solutions gave well above 40 kcounts s^{-1}, allowing size measurements within 20 s. The aluminium surface associated with the DLS measurements was anodized black to reduce the possibility of reflected light being collected by the detector. A section of the black surface can be seen in Fig. 2f. The channel surfaces not associated with DLS were not anodized black to improve the ability to visually monitor flow.

The DLS measurement provides autocorrelation functions as shown in Fig. 3. The measurements associated with larger particles are shifted to the right, decaying at longer delay times due to their slower rates of diffusion. The autocorrelation functions were fit by a mass weighted CONTIN function, which is commonly applied to polydisperse or multimodal samples.[33] The CONTIN function obtains decay rates through the use of an inverse Laplace transform. The decay modes are related to a diffusion coefficient, which in turn is related to the hydrodynamic diameter, D_H, with the Stokes–Einstein relation. The solvent viscosity and refractive index were taken as the mass-weighted mean of dodecane and other trace levels of components (*i.e.*, anisole and residual monomer) in the solvent.

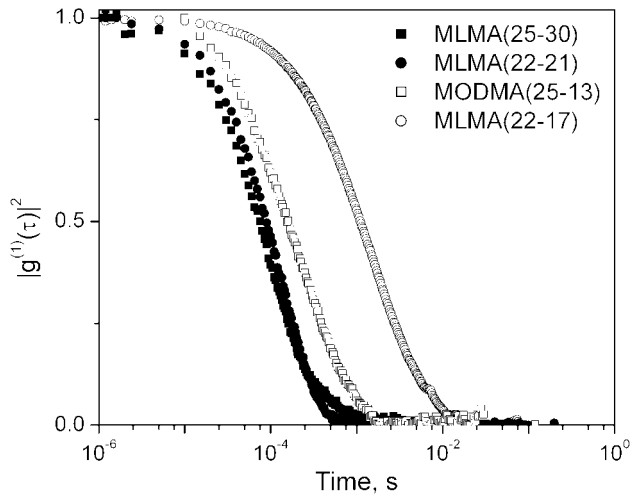

Fig. 3 Example autocorrelation functions for the block copolymers synthesized on a device and diluted with dodecane. The aggregated micelle samples, MODMA(25–13) and MLMA(22–17) decay at distinctly slower timescales, due the slower diffusion of the larger particles. The sample names denote the block molecular masses in kg mol^{-1}, *e.g.*, P(MMA)$_{249}$-*b*-P(LMA)$_{120}$ is termed MLMA(25–30).

4. Experimental

Materials

2-Phenylethyl bromide (PEBr, 97% purity), ethyl 2-bromoisobutylate (EBiB, 98% purity), methyl 2-bromopropionate (MBP), copper(I) bromide (CuBr, 99.999% purity), copper(I) chloride (CuCl, 99.995+% purity), pentamethyldiethylenetriamine (PMDETA, 99% purity), and 1,1,4,7,10,10-hexamethyltrienetetraamine (HMTETA, 97% purity) were purchased from Aldrich and were used as received. Styrene (St, 99% purity), methyl methacrylate (MMA, 99% purity), lauryl methacrylate (LMA, 96% purity), octadecyl methacrylate (ODMA, contained 35% cetyl methacrylate), benzyl methacrylate (BnMA, 96% purity), and butyl acrylate (BA, 99+% purity) were purchased from Aldrich, and were used after the inhibitor was removed by passing through an activated alumina column (aluminium oxide; Aldrich ≈150 mesh). Anisole (99,% purity) was purchased from Aldrich and used as received. Dodecane (≥90% purity) was purchased from Fluka and used as received.

Characterization

^{1}H nuclear magnetic resonance (NMR) spectra were recorded in $CDCl_3$ as a solvent on a JEOL 270 MHz spectrometer and were reported in parts per million (δ) from an internal tetramethylsilane (TMS) or residual solvent peak. The number average relative molecular mass (M_n) and polydispersity index: PDI ($= M_w/M_n$) of polymers were determined by gel permeation chromatography (GPC) using a Breeze HPLC System (Waters) equipped with a 1515 isocratic HPLC pump with online degassing, 717 Plus autosampler, 2414 refractive index detector, a guard column (ViscoGEL I-Series Columns; I-Guard-0478), and two mixed bed columns (ViscoGEL I-Series Columns; I-MBLMW-3078 and I-MBHMW-3078). The columns were calibrated by a series of polystyrene standards (Polymer Laboratories, EasiCal PS-2) and polymethyl methacrylate standards (Polymer Laboratories, EasiCal PM-1) at 40 °C in THF (flow rate; 1.0 mL min^{-1}).

Homopolymer synthesis

In a typical synthesis of PMMA homopolymer, two syringes were mounted on syringe pumps (Braintree Scientific), and were connected to a microfluidic device with Teflon tubes (I.D. = 790 μm, O.D. = 1.58 mm). The first syringe contained ethyl 2-bromoisobutylate (19.5 mg, 0.10 mmol) and methyl methacrylate (3003 mg (3.21 mL), 30 mmol) that had been gently degassed with Ar for 15 min. The second syringe contained a solution of copper(I) bromide (7.2 mg, 0.05 mmol) and anisole (3.21 mL) that also had been gently degassed with Ar for 15 min. Pentamethyldiethylenetriamine (PMDETA) (8.7 mg, 0.05 mmol) was added to this solution under Ar flow, followed by vigorous stirring or sonication until the copper complex was formed and dissolved completely. The product solution from the outlet of the device was collected (*ca.* 50 μL), and dissolved in air-saturated $CDCl_3$ or THF to measure ^{1}H NMR or gel permeation chromatography (GPC).[31]

Block copolymer synthesis

The main difference in producing diblock copolymers was the use of a macroinitiator, as is highlighted in Fig. 4. For example, synthesis of poly(methyl methacrylate-*b*-lauryl methacrylate) involved blending two solutions. The first solution comprised PMMA-Br (M_n = 21 800, PDI = 1.38; 440 mg, 0.020 mol), lauryl methacrylate (0.5 mL), and anisole (1.0 mL). The second solution comprised copper(I) bromide (5.7 mg, 0.04 mmol), lauryl methacrylate (1.0 mL), anisole (0.5 mL), and PMDETA (8.3 mg, 0.04 mmol). Both syringes contained LMA to prevent precipitation of the PMMA-Br macroinitiator upon blending the two solutions. In one case, a copper chloride catalyst was used because it is known to form block copolymers from bromine terminated macroinitiators with narrower polydispersity. The kinetics associated with this catalyst, however, are too slow to efficiently produce higher molecular weight materials within a microfluidic device. M_n of the diblock copolymer was determined from (M_n of PMMA macroinitiator determined by GPC, calibrated with PMMA standards, prior to copolymer synthesis) + (M_n of PLMA or PODMA estimated from the level of conversion determined by ^{1}H NMR of the product solution collected from the outlet of the device). GPC traces of the PMMA macroinitiator and the corresponding diblock copolymers did not appear to contain any shoulder peaks (see electronic supplementary information).† Table 1 lists the homopolymers and diblock copolymers synthesized with these

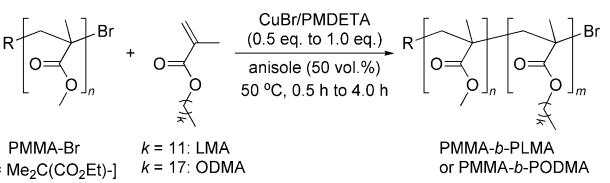

Fig. 4 ATRP block copolymerization using a PMMA macroinitiator.

Table 1 ATRP of homo- and block copolymers[a]

Entry	Abbreviation	Monomer/initiator[b]	Condition (equiv)	°C/min[c]	Conv.[d](%)	M_n[e]	PDI[e]
Homopolymers – batch reactions, for comparison							
1	PMMA[f]	MMA/EBiB	300	50/300	65	21 800	1.38
2	PMMA	MMA/EBiB	300	50/240	41	16 900	1.27
3	PMMA[g]	MMA/EBiB	1000	30/500	30	38 100	1.15
4	PMMA[g]	MMA/EBiB	1000	30/1030	80	94 400	1.35
Homopolymers – microfluidic							
5	PS	Styrene/PEBr	200	100/300	41	7200	1.19
6	PMMA	MMA/EBiB	300	50/110	22	5400	1.16
7	PMMA	MMA/EBiB	300	50/280	44	14 000	1.28
8	PLMA	LMA/EBiB	100	50/140	56	13 500	1.17
9	PODMA	ODMA/EBiB	100	50/200	80	11 700	1.25
10	PBnMA	BnMA/EBiB	300	40/120	47	26 200	1.25
11	PBA	BA/MBP	100	70/280	58	5900	1.13
12	PBA	BA/MBP	100	70/400	71	7300	1.15
Diblock copolymers – microfluidic						M_n[h]	PDI[e]
13	MLMA(25–30)[i]	LMA/PMMA-Br[j]	485[k]	50/65	25	55 300	1.44
14	MLMA(22–21)	LMA/PMMA-Br[l]	255	50/90	33	42 900	1.46
15	MODMA(25–13)	ODMA/PMMA-Br[j]	250[m]	90/270	15	37 700	1.31
16	MLMA(22–17)	LMA/PMMA-Br[l]	250	50/30	27	39 100	1.40

[a] CuBr/pentamethyldiethylenetriamine (PMDETA) complex (0.5–1.0 equiv) was used. Reactions were conducted in 50% anisole, by volume. [b] EBiB: ethyl 2-bromoisobutylate, MBP: methyl 2-bromopropionate, PEBr: 2-phenylethyl bromide. [c] Residence time = (total volume of microchannel)/(total flow rate). [d] Determined by ^{1}H NMR analysis of crude sample, which refers to the final product solution exiting from the device. [e] Determined by GPC analysis of crude sample. [f] Used as macroinitiator. [g] From literature, ref. 36. [h] Determined by both GPC and ^{1}H NMR analysis of crude sample.[31] [i] Numbers denote the block masses in kg mol^{-1}. [j] M_n = 24 900, PDI = 1.43. [k] *ca.* 4.0 equiv of CuBr catalyst was used. [l] M_n = 21 800, PDI = 1.38. [m] *ca.* 1.5 equiv of CuCl catalyst was used.

methods. The block copolymers are denoted based on the block masses in kg mol^{-1}.

5. Results and discussion

Microfluidic ATRP

Atom transfer radical polymerization (ATRP)[34,35] is a popular method because it is capable of producing a wide variety of polymers in a well controlled manner, and many of the initiators and catalysts are commercially available. In this work, ATRP was conducted on commonly used monomers to demonstrate the feasibility of producing materials in this way. In fact, styrene represents one of the harsher reaction conditions associated with ATRP, requiring long reaction times and elevated temperatures. The polymerization of styrene (St) was carried out at 100 °C to give polystyrene (PS) with a narrow PDI (1.19) in moderate yield (41%), as is shown in Table 1. Methacrylates represent another large class of monomers, and well defined PMMA was produced on-chip at 50 °C with narrow PDI (1.16, 1.28) in moderate yield (22% and 44%). In addition, well defined PLMA (PDI = 1.17, 56% conversion) and PODMA (PDI = 1.25, 80% conversion) were prepared. Polybenzyl methacrylate (PBnMA) was produced with controlled molecular weight and narrow polydispersity (1.25) at 40 °C, and demonstrates that certain monomers have relatively fast polymerization kinetics in ATRP. In addition, polybutyl acrylates (PBA) were prepared with a narrow PDI (1.13, 1.15) and were conducted to relatively high conversion (71%). All of these polymers are described in Table 1, entries 5–12. A Cu/PMDETA catalyst complex was employed in this work due to its common use in ATRP. An advantage of this complex is that it tends to have faster reaction kinetics than other available catalysts. Cu/PMDETA is generally considered to be a heterogeneous catalyst, but in the conditions employed in this work, Cu/PMDETA was found to dissolve well. Nevertheless, a purely homogeneous catalyst may control the polymerization better due to its decreased sensitivity to mixing. Also, it should be noted that the aluminium oxide surface of the devices could potentially degrade the catalyst. While this was not observed to be a problem in this work, it could be addressed, if it occurred, by using stainless steel. Given the success of these representative monomers and reaction conditions, it is expected that these devices are compatible with most, if not all, of the wide variety of ATRP reactions.

PMMA-*b*-PLMA and PMMA-*b*-PODMA were also produced on a device. The conversion of the copolymers was kept relatively low to maintain a low solution viscosity, which increased noticeably at higher conversions due to the higher molecular weight of the copolymers. The composition of the diblock copolymers was varied from a MMA mass fraction of $0.45 < f_{MMA} < 0.66$, as listed in Table 2, because this composition range encompasses corresponding solutions with both stable discrete micelles and unstable aggregated micelles.

The macroinitiators used to prepare the copolymers were made in batch reactors, and had a somewhat broad polydispersity. Growth of the second block within the microchannel, however, did not significantly broaden the polydispersity of the final copolymer. Work by Ramakrishnan, *et al.* observed that the polydispersity of PMMA broadens with conversion (Table 1, entries 3,4),[36] and the polydispersity of the macrointiators was likely caused by preparing them at relatively high conversions (65%, Table 1, entry 1). In general, comparison of PMMA synthesis in microchannels and batch reactors shows no discernable difference. Table 1 lists values obtained within the devices (entries 6,7) and batch reactors (entries 1–4). In this work on PMMA, the PDI was narrow (≤1.28) at low conversions (22%

Table 2 Self-assembly of the block copolymers in dodecane

Abbreviation	Polymer	f_{MMA}[a]	% conc.[b]	$D_{H,MAX}$[c]/nm	Agg.[d]
MLMA(25–30)	$P(MMA)_{249}$-*b*-$P(LMA)_{120}$	0.45	6.7	28	No
MLMA(22–21)	$P(MMA)_{218}$-*b*-$P(LMA)_{83}$	0.51	3.3	35	No
MODMA(25–13)	$P(MMA)_{249}$-*b*-$P(ODMA)_{38}$	0.66	5.2	21, 330	Yes
MLMA(22–17)	$P(MMA)_{218}$-*b*-$P(LMA)_{68}$	0.56	3.1	550	Yes

[a] Mass fraction of PMMA. [b] Polymer concentration, mass%. Polymers were sufficiently diluted in dodecane to avoid multiple scattering. [c] The hydrodynamic diameter associated with the maximum CONTIN weighting. MODMA(25–13) had a bimodal distribution, and MLMA(22–17) had a broad distribution. [d] Aggregated micelles.

to 44%), and the PDI broadened ($\geq$1.35) at higher conversions (65% to 80%). This equivalence of batch and microfluidic based ATRP agrees with previous findings in our laboratory.[16,17]

Copolymers of MMA with LMA (or ODMA) represent a promising class of steric stabilizers that can be used in non-aqueous dispersion polymerization of PMMA latex. The pendent alkyl groups on LMA and ODMA have been proposed as simple replacements for traditionally used comb polymers produced from poly(12-hydroxy steric acid) and MMA.[37,38] In addition, it is expected that these synthesis and analysis methods can, in general, be extended to amphiphilic block copolymer micelles, which are finding increasing use in biomedical research.[2]

The ATRP reactions used in this work required as long as 6 h to complete. This highlights the ruggedness of the devices with respect to reactions requiring demanding chemicals, temperatures, and reaction times, and possess sensitivity to trace levels of oxygen and water. A potentially valuable application of this device is in automated sequential analysis (*e.g.*, high-throughput screening) of nanostructured materials, as has been described elsewhere.[3,16,17] The robustness of this device eliminates limitations in selecting appropriate synthetic methods for producing materials with interesting nanoscale structure. It should be pointed out that sequential analysis, in general, is more convenient for fast reactions, and these are preferable if they can produce a material of interest.

On the other hand, these miniaturized reactors possess several intrinsic advantages, such as improved heat transfer and the ability to influence mixing, and these advantages can be exploited to improve some polymerizations. One such polymerization may be living anionic polymerization, which could benefit from improved heat transfer and mixing because it is highly exothermic and has rapid polymerization kinetics. Work on this topic is underway.

Micelle formation

The examined copolymers self-assemble in dodecane because it preferentially solvates the PLMA (or PODMA) blocks. Dodecane is a non-solvent for PMMA. Thus, micelles with PMMA cores and PLMA (or PODMA) coronas form. It should be noted that residual amounts of unreacted LMA (or ODMA) are present in the final solution. This monomer is expected to disperse in the dodecane, without impacting micelle formation. Initial evaluation of on-chip ATRP involved diluting the synthesized polymers offline in dodecane and measuring them in a full-scale DLS device. These are MLMA(22–21) and MLMA(22–17), listed in Table 2. Once the micelle behavior of the polymers was verified, dilution and DLS of MLMA(25–30) and MODMA(25–13) were conducted on a single integrated device as depicted in Fig. 1. The polymers were sufficiently diluted to avoid multiple scattering. The fiber optic DLS allowed for relatively high concentrations (listed in Table 2) to be observed because the close proximity of the laser and detector probes reduced multiple scattering. In addition, DLS is sensitive to large particles, which can arise from trace amounts of precipitated polymer or decomposed catalyst. It was found that filtering the crude reaction solution in line with a 0.45 μm filter was sufficient to eliminate scattered signal not associated with the micelles (Fig. 1). In this work, unfiltered samples were measured, and subsequently filtered only when no obvious levels of micelle aggregates were present. That is, the filtering did not remove aggregated micelles, but instead allowed for improved quantitative data fitting of unaggregated micelle samples. In addition, homogeneously dissolved catalyst passed through the filter, but removing this low level of catalyst (<0.01 mol%) by passing the solution through alumina was not found to influence micelle formation. The catalyst, however, may present challenges for other spectroscopic tools, and inline alumina columns may possibly be of benefit in these cases.

Micelle evaluation

The micelle sizes measured with the integrated fiber optic DLS were found to agree well with those measured offline. Fig. 5 shows that a unimodal distribution of micelles was observed for MLMA(25–30) and MLMA(22–21), and a bimodal distribution corresponding to single and aggregated micelles was observed for MODMA(25–13). A broad polydisperse distribution was observed for MLMA(22–17). These results suggest that the copolymer composition strongly influences whether the micelles aggregate into clusters. That is, the block copolymer micelles are highly susceptible to aggregation when the corona block is insufficiently long (*i.e.*, $f_{MMA} \geq 0.56$). Table 2 lists the composition of the copolymers and whether the micelles aggregated. Noting that MODMA(25–13) was closer to having discrete micelles than MLMA(22–17) despite having a higher f_{MMA} suggests that the PODMA block was more effective in stabilizing the PMMA core than PLMA. These observations of micelle aggregation and of the significance of copolymer composition are consistent with previous observations of PS-*b*-PODMA in dodecane.[39,40]

In addition, CONTIN analysis provides a quantitative means of evaluating particle size and size distribution. In general, DLS is well suited to quantitatively evaluate samples with well defined particle sizes. For example, comparing MLMA(25–30)

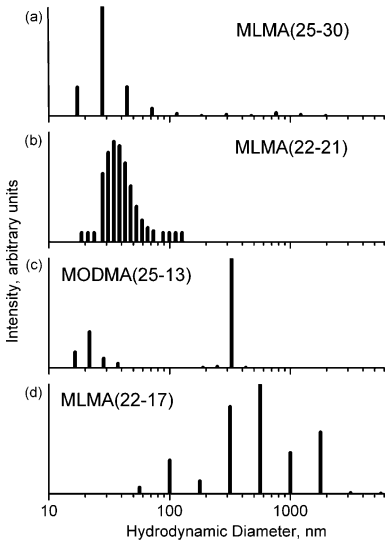

Fig. 5 Particle size distributions measured with DLS, obtained from mass weighted CONTIN fits. (a,b) Micelles formed with no micelle aggregates, $f_{MMA} = 0.45$, 0.51, respectively. (c) A bimodal distribution of micelles and aggregated micelles, $f_{MMA} = 0.66$, and (d) a broad distribution of aggregates $f_{MMA} = 0.56$. The histograms correspond to data obtained with (a,c) miniaturized DLS, (b,d) traditional full-scale DLS.

and MLMA(22–21) in Fig. 5a,b shows them to approximately have the same average size given the resolution of the histogram. Micelles formed by MODMA(25–13) appear to be slightly smaller, but the fitting could be slightly skewed by the presence of micelle aggregates. On the other hand, the ability of DLS to evaluate very polydisperse samples is limited, as can be seen in Fig. 5d. This is in part caused by the strong dependence of scattering strength on particle size, making contributions from smaller components difficult to discern. That is, MLMA(22–17) likely had some level of discrete micelles, whose scattering contribution is overwhelmed by the large amount of aggregated micelles. Nevertheless, DLS provides a very clear distinction between samples containing aggregated and discrete micelles.

A limitation of this integrated device is that the DLS does not measure the molecular weight of the polymer products, thus requiring offline analysis with ^{1}H NMR and GPC. A potential improvement would be to integrate methods for molecular weight determination directly onto the device. For example, monitoring of parallel microfluidic flow streams has successfully been used to determine molecular weights.[9] Also, static light scattering, which measures M_w, can likely be integrated onto microfluidic devices given that it has long been used as a flow through GPC detector. It should be noted, however, that when producing nanoparticles, instead of block copolymers, the products can be fully characterized with DLS alone, thereby eliminating the need for either offline analyses or integration of additional measurement techniques.

6. Conclusions

This work has developed a new simple low-cost metal-based microfluidic device compatible with the synthesis of common synthetic polymers, including polystyrene and several poly(meth)acrylates. ATRP reactions were conducted to form these homopolymers as well as block copolymers. The block copolymers were diluted on the device with a selective solvent to induce micelle formation, and the size of the micelles was determined with integrated fiber optic dynamic light scattering (DLS). This approach seamlessly integrates synthesis, processing, and analysis of polymers. Moreover, miniaturization of the DLS, which was reduced to a measurement volume of 4 μL, simplified alignment, eliminated complications with refraction, and reduced multiple scattering. This DLS tool can also be used for more straightforward analyses, such as turbidity and fluorescence intensity measurements. The PMMA-*b*-PLMA and PMMA-*b*-PODMA copolymers were found to form discrete micelles ($D_H = 20$ nm to 30 nm) when the corona block was sufficiently long (*i.e.*, $f_{MMA} < 0.51$), otherwise the micelles aggregated. The polymerizations employed in this work were relatively demanding in terms of the required chemicals, temperatures, and reaction times. It is therefore expected that these devices will be applicable to a wide variety of polymerizations. Given the integrated DLS, microfluidic synthesis and characterization of other nanostructured materials, including vesicles, polymer-coated hybrid nanoparticles, and latexes, promises to be important further application of this work.

Acknowledgements

T.Q.C. was supported by a NIST/National Research Council Postdoctoral Associateship. This work was carried out at the NIST Combinatorial Methods Center (www.nist.gov/combi). Official contribution of NIST; not subject to copyright in the United States.

References

1 N. Hadjichristidis, S. Pispas and G. Floudas, *G. Block, copolymers : synthetic strategies, physical properties, and applications*, Wiley, Hoboken, 2003.
2 G. Riess, *Prog. Polym. Sci.*, 2003, **28**, 1107.
3 E. Amis, *J. Nat. Mater.*, 2004, **3**, 83.
4 Z. H. Nie, W. Li, M. Seo, S. Q. Xu and E. Kumacheva, *J. Am. Chem. Soc.*, 2006, **128**, 9408.
5 R. F. Shepherd, J. C. Conrad, S. K. Rhodes, D. R. Link, M. Marquez, D. A. Weitz and J. A. Lewis, *Langmuir*, 2006, **22**, 8618.
6 A. Manz, D. J. Harrison, E. M. J. Verpoorte, J. C. Fettinger, H. Ludi and H. M. Widmer, *Chimia*, 1991, **45**, 103.
7 T. Vilkner, D. Janasek and A. Manz, *Anal. Chem.*, 2004, **76**, 3373.
8 J. Atencia and D. J. Beebe, *Nature*, 2005, **437**, 648.
9 C. D. Costin and R. E. Synovec, *Anal. Chem.*, 2002, **74**, 4558.
10 P. Guillot, P. Panizza, J. B. Salmon, M. Joanicot, A. Colin, C. H. Bruneau and T. Colin, *Langmuir*, 2006, **22**, 6438.
11 A. I. Norman, W. H. Zhang, K. L. Beers and E. J. Amis, *J. Colloid, Interface Sci.*, 2006, **299**, 580.
12 C. L. Kuyper, K. L. Budzinski, R. M. Lorenz and D. T. Chiu, *J. Am. Chem. Soc.*, 2006, **128**, 730.
13 P. S. Dittrich and A. Manz, *Anal. Bioanal. Chem.*, 2005, **382**, 1771.
14 B. J. Berne, R. Pecora, *Dynamic, Light Scattering*, Dover, Mineola, 2nd edn, 2000.
15 T. Q. Chastek, K. L. Beers and E. Amis, *J. Rev. Sci. Instrum.*, 2007, **78**, 072201.
16 T. Wu, Y. Mei, J. T. Cabral, C. Xu and K. L. Beers, *J. Am. Chem. Soc.*, 2004, **126**, 9880.
17 T. Wu, Y. Mei, C. Xu, H. C. M. Byrd and K. L. Beers, *Macromol. Rapid Commun.*, 2005, **26**, 1037.
18 P. J. A. Kenis, R. F. Ismagilov, S. Takayama, G. M. Whitesides, S. L. Li and H. S. White, *Acc. Chem. Res.*, 2000, **33**, 841.
19 Y. N. Xia and G. M. Whitesides, *Agnew. Chem., Int. Ed.*, 1998, **37**, 551.

20 H. Becker and L. E. Locascio, *Talanta*, 2002, **56**, 267.
21 J. N. Lee, C. Park and G. M. Whitesides, *Anal. Chem.*, 2003, **75**, 6544.
22 V. Hessel and H. Lowe, *Chem. Eng. Technol.*, 2003, **26**, 13.
23 V. Hessel and H. Lowe, *Chem. Eng. Technol.*, 2003, **26**, 391.
24 T. Iwasaki and J. Yoshida, *Macromolecules*, 2005, **38**, 1159.
25 A. Nagaki, K. Kawamura, S. Suga, T. Ando, M. Sawamoto and J. Yoshida, *J. Am. Chem. Soc.*, 2004, **126**, 14702.
26 K. Jahnisch, V. Hessel, H. Lowe and M. Baerns, *Agnew. Chem., Int. Ed.*, 2004, **43**, 406.
27 B. Mason, K. Price, J. Steinbacher, A. Bogdan and D. McQuade, *Chem. Rev.*, 2007, **107**, 2300.
28 P. D. I. Fletcher, S. J. Haswell, E. Pombo-Villar, B. H. Warrington, P. Watts, S. Y. F. Wong and X. L. Zhang, *Tetrahedron*, 2002, **58**, 4735.
29 Equipment and instruments or materials are identified in the paper in order to adequately specify the experimental details. Such identification does not imply recommendation by NIST, nor does it imply the materials are necessarily the best available for the purpose.
30 J. A. McGeough, *Micromachining, of Engineering Materials*, CRC, New York, 2002.
31 The standard uncertainty associated with this measurement is 5%.
32 H. S. Dhadwal and B. Chu, *Rev. Sci. Instrum.*, 1989, **60**, 845.
33 S. W. Provencher, *Comput. Phys. Commun.*, 1982, **27**, 229.
34 K. Matyjaszewski and J. H. Xia, *Chem. Rev.*, 2001, **101**, 2921.
35 S. H. Qin, J. Saget, J. R. Pyun, S. J. Jia, T. Kowalewski and K. Matyjaszewski, *Macromolecules*, 2003, **36**, 8969.
36 A. Ramakrishnan and R. Dhamodharan, *Macromolecules*, 2003, **36**, 1039.
37 H. V. Harris and S. J. Holder, *Polymer*, 2006, **47**, 5701.
38 G. Street, D. Illsley and S. J. Holder, *J. Polym. Sci., Part A: Polym. Chem.*, 2005, **43**, 1129.
39 M. Pitsikalis, E. Siakali-Kioulafa and N. Hadjichristidis, *Macromolecules*, 2000, **33**, 5460.
40 M. Pitsikalis, E. Siakali-Kioulafa and N. Hadjichristidis, *J. Polym. Sci., Part A: Polym. Chem.*, 2004, **42**, 4177.